

Degradation mechanisms of Ti/Al/Ni/Au-based Ohmic contacts on AlGaIn/GaN HEMTs

Ya-Hsi Hwang, Shihyun Ahn, Chen Dong, Weidi Zhu, Byung-Jae Kim, Lingcong Le, Fan Ren, Aaron G. Lind, James Dahl, Kevin S. Jones, Stephen J. Pearton, Ivan I. Kravchenko, and Ming-Lan Zhang

Citation: *Journal of Vacuum Science & Technology B* **33**, 031212 (2015); doi: 10.1116/1.4919237

View online: <http://dx.doi.org/10.1116/1.4919237>

View Table of Contents: <http://scitation.aip.org/content/avs/journal/jvstb/33/3?ver=pdfcov>

Published by the AVS: Science & Technology of Materials, Interfaces, and Processing

Articles you may be interested in

[Ti/Al/Ti/Ni/Au ohmic contacts on AlGaIn/GaN high electron mobility transistors with improved surface morphology and low contact resistance](#)

J. Vac. Sci. Technol. B **32**, 011216 (2014); 10.1116/1.4862165

[Analysis of surface roughness in Ti/Al/Ni/Au Ohmic contact to AlGaIn/GaN high electron mobility transistors](#)

Appl. Phys. Lett. **97**, 062115 (2010); 10.1063/1.3479928

[Ohmic contact formation mechanism of Ta/Al/Mo/Au and Ti/Al/Mo/Au metallizations on AlGaIn/GaN HEMTs](#)

J. Vac. Sci. Technol. B **23**, 2330 (2005); 10.1116/1.2101691

[Annealing temperature stability of Ir and Ni-based Ohmic contacts on AlGaIn/GaN high electron mobility transistors](#)

J. Vac. Sci. Technol. B **22**, 2635 (2004); 10.1116/1.1814111

[Correlation of contact resistance with microstructure for Au/Ni/Al/Ti/AlGaIn/GaN ohmic contacts using transmission electron microscopy](#)

J. Appl. Phys. **89**, 3143 (2001); 10.1063/1.1347003



Instruments for Advanced Science

| | | | | |
|---|--|--|--|--|
| <p>Contact Hiden Analytical for further details: W www.HidenAnalytical.com E info@hiden.co.uk</p> <p>CLICK TO VIEW our product catalogue</p> |  <p>Gas Analysis</p> <ul style="list-style-type: none"> › dynamic measurement of reaction gas streams › catalysis and thermal analysis › molecular beam studies › dissolved species probes › fermentation, environmental and ecological studies |  <p>Surface Science</p> <ul style="list-style-type: none"> › UHV TPD › SIMS › end point detection in ion beam etch › elemental imaging - surface mapping |  <p>Plasma Diagnostics</p> <ul style="list-style-type: none"> › plasma source characterization › etch and deposition process reaction › kinetic studies › analysis of neutral and radical species |  <p>Vacuum Analysis</p> <ul style="list-style-type: none"> › partial pressure measurement and control of process gases › reactive sputter process control › vacuum diagnostics › vacuum coating process monitoring |
|---|--|--|--|--|

Degradation mechanisms of Ti/Al/Ni/Au-based Ohmic contacts on AlGaIn/GaN HEMTs

Ya-Hsi Hwang, Shihyun Ahn, Chen Dong, Weidi Zhu, Byung-Jae Kim, Lingcong Le, and Fan Ren^{a)}

Department of Chemical Engineering, University of Florida, Gainesville, Florida 32611

Aaron G. Lind, James Dahl, Kevin S. Jones, and Stephen J. Pearton

Materials Science and Engineering, University of Florida, Gainesville, Florida 32611

Ivan I. Kravchenko

Center for Nanophase Materials Sciences, Oak Ridge National Laboratory, Oak Ridge, Tennessee 37830

Ming-Lan Zhang

Department of Electronic Science and Technology, Hebei University of Technology, Tianjin, 300401, China

(Received 13 February 2015; accepted 13 April 2015; published 27 April 2015)

The degradation mechanism of Ti/Al/Ni/Au-based Ohmic metallization on AlGaIn/GaN high electron mobility transistors upon exposure to buffer oxide etchant (BOE) was investigated. The major effect of BOE on the Ohmic metal was an increase of sheet resistance from 2.89 to 3.69 Ω/\square after 3 min BOE treatment. The alloyed Ohmic metallization consisted 3–5 μm Ni-Al alloy islands surrounded by Au-Al alloy-rings. The morphology of both the islands and ring areas became flatter after BOE etching. Energy dispersive x-ray analysis and Auger electron microscopy were used to analyze the compositions and metal distributions in the metal alloys prior to and after BOE exposure. © 2015 American Vacuum Society. [<http://dx.doi.org/10.1116/1.4919237>]

I. INTRODUCTION

The performance of AlGaIn/GaN high electron mobility transistors (HEMT) has made remarkable progress in recent years, showing great promise for applications such as military radar and satellite-based communications systems.^{1,2} Due to the large energy bandgap of GaN (3.26 eV) and high breakdown field, these devices are well-suited to high power applications. However, due to this large bandgap, it is difficult to create a low resistance Ohmic metal on nitride HEMTs. The typical Ohmic contact used is a Ti/Al/Ni/Au metal stack annealed at 800–850 °C in N₂ ambient. By changing the annealing temperature or time,³ a contact resistance of $3.22 \times 10^{-7} \Omega/\text{cm}^2$ was achieved for Ti/Al/Ni/Au metal stacks to AlGaIn/GaN HEMT. These data are reported for measurement right after annealing and without exposure to chemicals that are part of subsequent processing steps. During the fabrication process, these contacts might be exposed to a number of chemicals, including buffered oxide etchant (BOE) which is an acidic buffered solution. As a result, it is important to know the performance change of Ohmic metal and possible degradation mechanisms after such BOE exposure.

BOE is a typical etchant to remove the native oxide or passivation layers such as silicon oxide or silicon nitride.⁴ It is a mixture of HF and NH₄F, which gives a stable etching performance by acting as a buffering agent to maintain pH. Based on their standard electrode potentials, most of the metals including Ti, Al, and Ni are anodic and will react with acid solution to form hydrogen gas.^{5,6} The etching rate of HF for sputtered Ti was reported to be faster than 10 kÅ/min.⁶ For another common contact metal, Al, the

etching rate in 5:1 BOE solutions was reported to be 11 nm/min.⁷ The etching rate of 5:1 BOE solution for Ni and Au is almost zero.⁷ During the opening of the passivation layer on HEMTs, the Ohmic metal is exposed to the BOE solution and it is inevitable it will react with HF. As a result, care must be taken to open the passivation window but not damage the Ohmic metal.

There is no study on changes in Ohmic metal performance of Ti/Al/Ni/Au contacts on nitride HEMTs after BOE treatment. Therefore, it is important to study this performance change after BOE treatment. In this work, we monitored the resistance change of Ti/Al/Ni/Au Ohmic metal when exposed to BOE by four point probe measurements. After treatment, energy dispersive x-ray spectroscopy (EDX) and Auger analysis were used to quantitatively determine the composition change. Possible mechanisms are discussed to explain the performance changes after BOE treatment.

II. EXPERIMENT

HEMT structures were grown on Si substrates using a metal organic chemical vapor deposition system, starting with a thin AlN nucleation layer followed with a 2 μm low-defect carbon-doped GaN buffer layer, a 23 nm undoped GaN layer, and a 21.2 nm undoped AlGaIn layer with a 18% Al mole fraction and capped with a 2.5 nm undoped GaN layer. Ohmic contact was deposited with a standard lift-off e-beam evaporated Ti/Al/Ni/Au (45/125/45/100 nm) based metallization, and the samples were subsequently annealed at 850 °C for 1 min under N₂ ambient. After annealing at 850 °C for 1 min under a N₂ ambient, the sheet resistance of

^{a)}Electronic mail: fren@che.ufl.edu

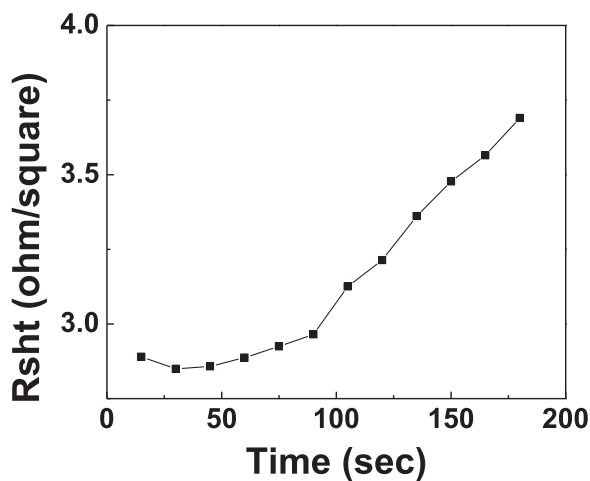


FIG. 1. Sheet resistance of alloyed Ti/Al/Ni/Au-based Ohmic metallization as a function of BOE treatment time measured with the four point probe technique.

the Ohmic metal from four point probe measurements was around $2.7 \Omega/\square$.

The wafer with Ti/Al/Ni/Au Ohmic metal was diced into several pieces and treated in BOE at different time, with the

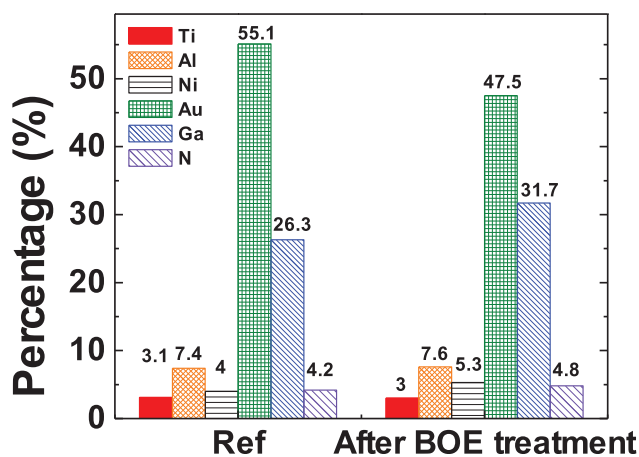


FIG. 2. (Color online) Percentages of metal elements in alloyed Ti/Al/Ni/Au metallization prior to and after 200 s of BOE treatment, measured by EDX spectroscopy.

sheet resistance being monitored by four point probe measurements. Scanning electron microscope (SEM) with either backscattering electron detector or secondary electron detector was used to examine the surface morphology change

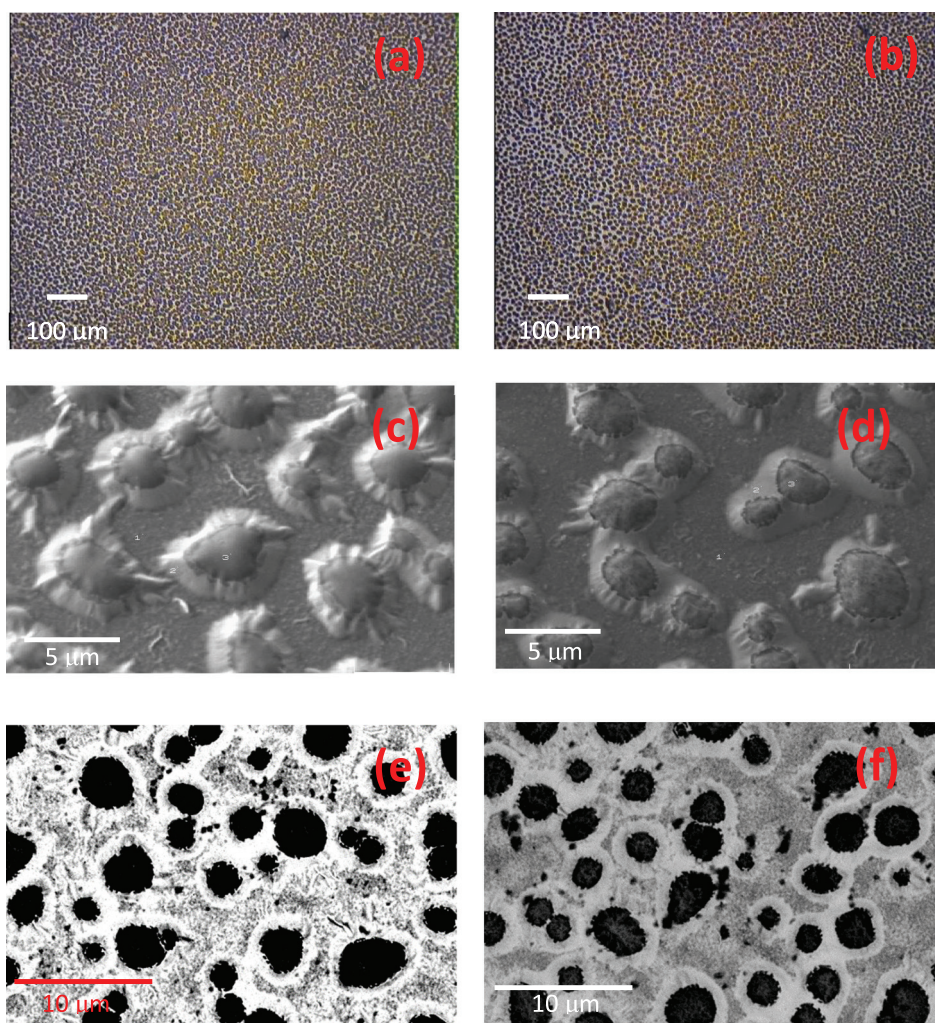


FIG. 3. (Color online) Morphologies of alloyed Ti/Al/Ni/Au metallization (a) prior to and (b) after 200 s of BOE treatment examined with optical microscopy. SEM pictures of alloyed Ti/Al/Ni/Au metallization (c) prior to and (d) after 200 s of BOE treatment using a secondary electron detector. SEM pictures of alloyed Ti/Al/Ni/Au metallization (e) prior to and (f) after 200 s of BOE treatment using a backscattering electron detector.

before and after BOE treatment. EDX was used to quantify the composition change before and after BOE treatment. Finally, Auger depth profiling was used to analyze the composition within the metal film.

III. RESULTS AND DISCUSSION

Figure 1 shows the sheet resistance (R_{sh}) of alloyed Ti/Al/Ni/Au Ohmic metallization as a function of BOE treatment time. The metal sheet resistance gradually increased from 2.7 to 3.7 Ω/\square after 200 s of BOE treatment. The BOE solution was composed of a 6:1 volume ratio of 40% NH_4F in water to 49% HF in water. Au should be inert in BOE. However, since the standard reduction potentials of Ti, Al, and Ni are all negative, oxidation and dissolution processes are favorable for these three metals and thus increase metal sheet resistance after treatment in BOE.

Broad area EDX scan was used to estimate the rough composition change of alloyed Ohmic metallization after BOE treatment, as shown in Fig. 2, and the composition of each element was averaged for individual content across an area of $30\ \mu\text{m} \times 30\ \mu\text{m}$. For EDX analyses, the intensity of the x-ray beam generated is proportional to the incident electron beam current and the atomic mass of an element. Heavier elements, such as Au, are much easier to detect than lighter elements (Al) and will have a higher x-ray yield. Therefore, Au would be overestimated in this mixed metallization. However, as shown in Fig. 2, Au unexpectedly decreased by around 7% and Ga increased by 4%. The content of Ti decreased by 0.1% and the contents for the rest of elements, Al, Ni, and N, increased by 0.2%, 1.3%, and 0.6%, respectively. For EDX, the x-rays are generated in a region about $2\ \mu\text{m}$ in depth of the sample. The thickness of the Ti/Al/Ni/Au Ohmic metallization was around $0.3\ \mu\text{m}$,

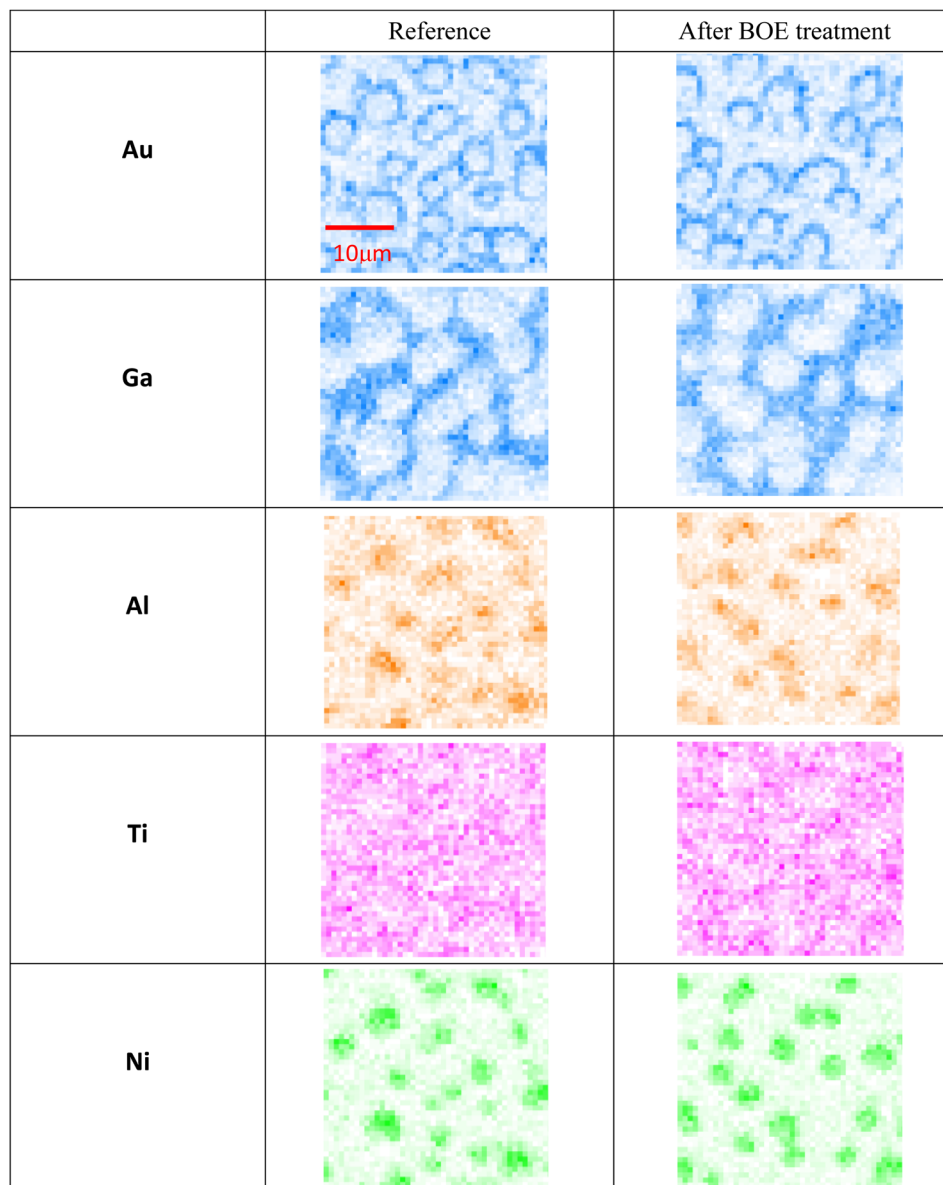


FIG. 4. (Color online) EDX elemental mappings of alloyed Ti/Al/Ni/Au metallization prior to and after 200 s of BOE treatment.

and thus, the EDX signals of Ga and N should be dominated by the bulk GaN even with some Ga or N out-diffusing through the alloyed Ohmic metallization. Thus, it is reasonable to assume that the Ga and N contents did not change significantly. The percent increases of Ga and N content after BOE treatment were due to the decrease of the Au content. By comparing the increases of percent content of Al, it was less than the percent increase of Ga or N. Therefore, besides Ti and Au, the content of Al also decreased after BOE treatment. However, the increase of Ti/Al/Ni/Au Ohmic metallization sheet resistance should be mainly caused by the decrease of Au content in the BOE treated sample. Although Au is inert to BOE, Au in the ring area could be removed by the etching of Al underneath this layer.

Figure 3 shows optical microscope pictures of alloyed Ohmic metallization before and after BOE treatment, and

pictures for the same samples taken with SEM using a secondary electron detector as well as a backscattering electron detector. There were no clear differences for the pictures taken with the optical microscope between [Fig. 3(a)] the reference and [Fig. 3(b)] BOE treated sample, and both pictures exhibited very rough surface morphology across the entire alloyed Ohmic metallization. However, the SEM pictures using the secondary electron detector clearly exhibited three distinct regions on the alloyed Ohmic metallization. There were islands bulging up and surrounded by a ring, and there was a flat surface between these islands. The SEM pictures also revealed a couple of distinct differences between Fig. 3(c) the reference and Fig. 3(d) BOE treated samples. First, the surface of the islands was etched and became rougher after BOE treatment. Besides etching the surface of islands, those rings surrounding the islands also got etched and became narrower. The height of islands was reduced from around 300 to 200–250 nm after BOE treatment measured from the field region on the Ohmic metal with an Alpha-Step profiler. Further, SEM pictures taken with backscattering electron detector also exhibited three distinct regions on the alloyed Ohmic metallization; dark color black

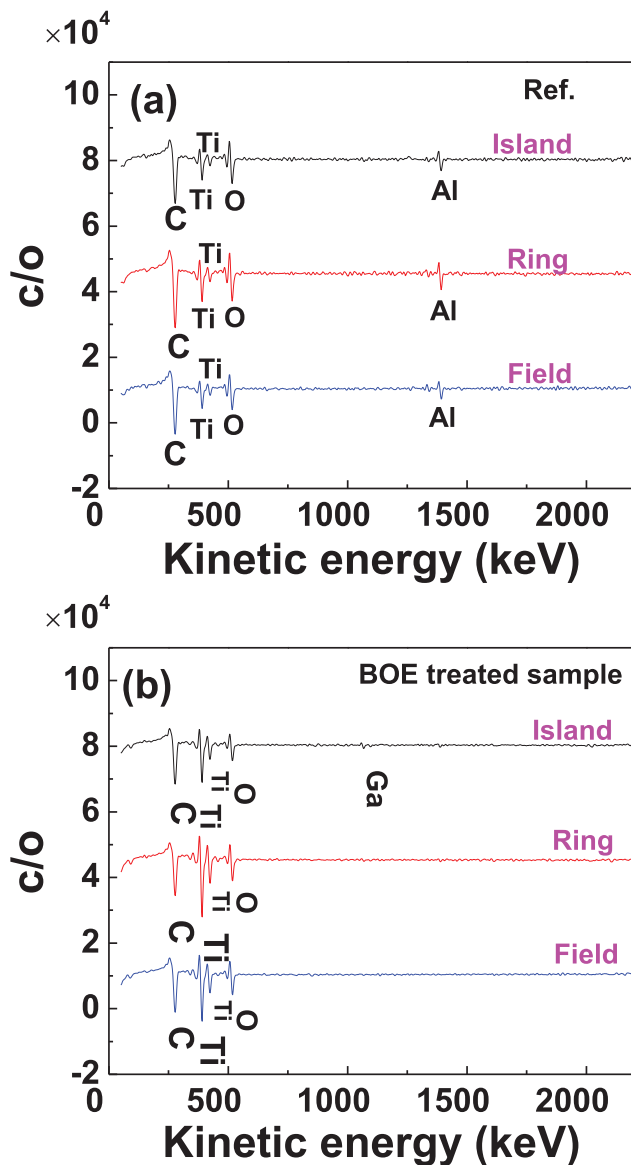


FIG. 5. (Color online) Auger surface scan analyses of island, ring and field regions for (a) untreated sample and (b) BOE treated sample.

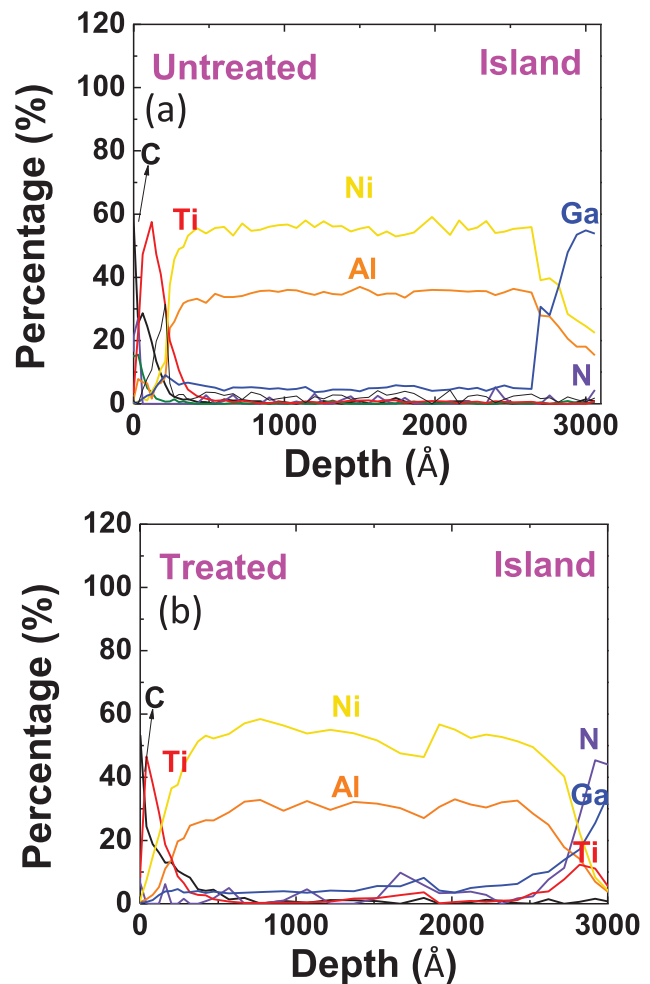


FIG. 6. (Color online) Auger depth profile of the island area on (a) untreated sample and (b) BOE treated sample.

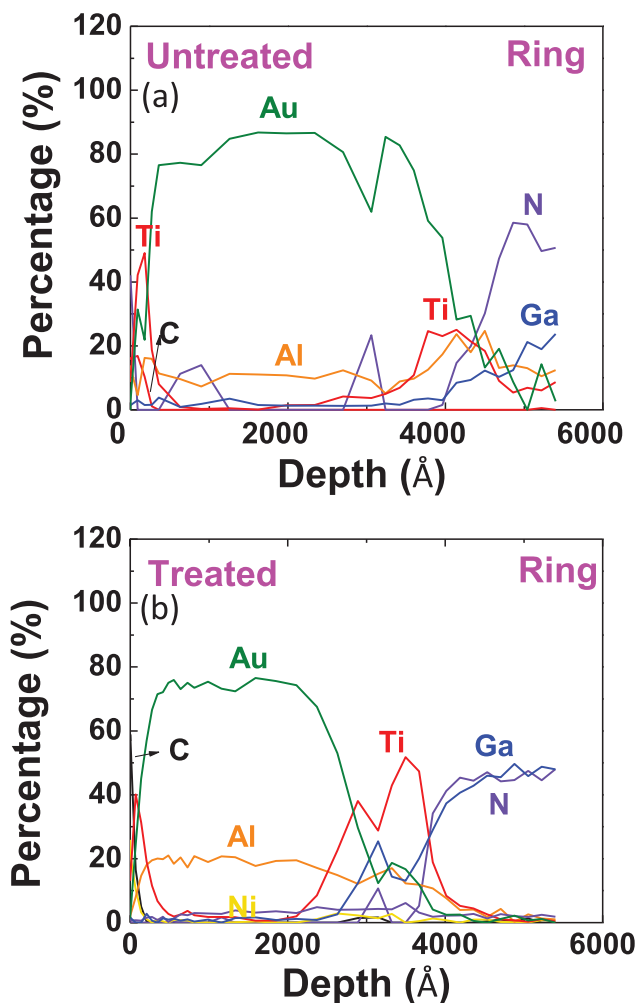


Fig. 7. (Color online) Auger depth profile of the ring area (a) untreated sample and (b) BOE treated sample.

islands surrounded by a brighter ring, and islands connected with a gray color area, as shown in Figs. 3(e) and 3(f). The signal intensities detected by the backscattering electron detector are proportional to the atomic numbers; the brighter areas are dominated by heavier elements, such as Au in our system, and the darker areas should comprise lighter elements, such as Al. Thus, those darker color islands ranging from 3 to 5 μm must have Al, Ni and Ti bounded by a $\sim 1 \mu\text{m}$ wide ring containing Au. The gray color region, defined as the field region, could have both a heavier element, Au, as well as lighter elements, Al, Ti, and Ni. It was reported that Ni-Al intermetallic phases react to form bumps and are bounded by Au-Al intermetallic phases.⁸ Based on these results, some of the Al and Ga were etched off by BOE. Au in the ring area could be removed by the etching of Al underneath this layer.

Figure 4 illustrates the EDX mapping of Au, Ga, Al, Ti, and Ni for reference and BOE treated samples. Al and Ni are mainly located in those islands, and Au and Ga mostly contained in the ring and field areas, respectively. Ti, on the other hand, is uniformly dispensed in the ring and field areas and scattered in the islands. After BOE treatment, the contrast between Au-based rings and the island areas became

less obvious, which was consistent with the results obtained by SEM. The intensities of the Ga signal in the ring areas also decreased after BOE treatment. The Al signal generally decreased for the entire areas, which was in line with Auger surface scan result shown in Fig. 5. For the as-alloyed sample, Ti, Al, carbon (C), and oxygen (O) were present on the surface for all three regions. After BOE treatment, Al was removed and Ga was detected in the island areas.

To investigate the depth-dependent composition of alloyed Ti/Al/Ni/Au Ohmic metallization in island, ring and field regions between islands, Auger depth profiling analyses were performed. Figure 6(a) shows the Auger depth profiling of the island area on the untreated sample. The surface region consisted of C, O, Ti, and Al, followed with a 40 nm Ti layer and a layer of 200 nm Ni-Al alloy. Ga clearly diffused throughout the Ni-Al alloy and Ti layer. It has previously been reported that a Ni-Al intermixing layer in these types of contacts was formed after annealing to minimize the interfacial energy.^{9,10} After BOE treatment, the surface Al was removed, as shown in Fig. 6(b). There was no clear effect of BOE treatment on both Ti and Ni-Al alloy layer. However, there was a Ti peak appearing at the Ni-Al alloy and GaN interface for the reference sample, which was not

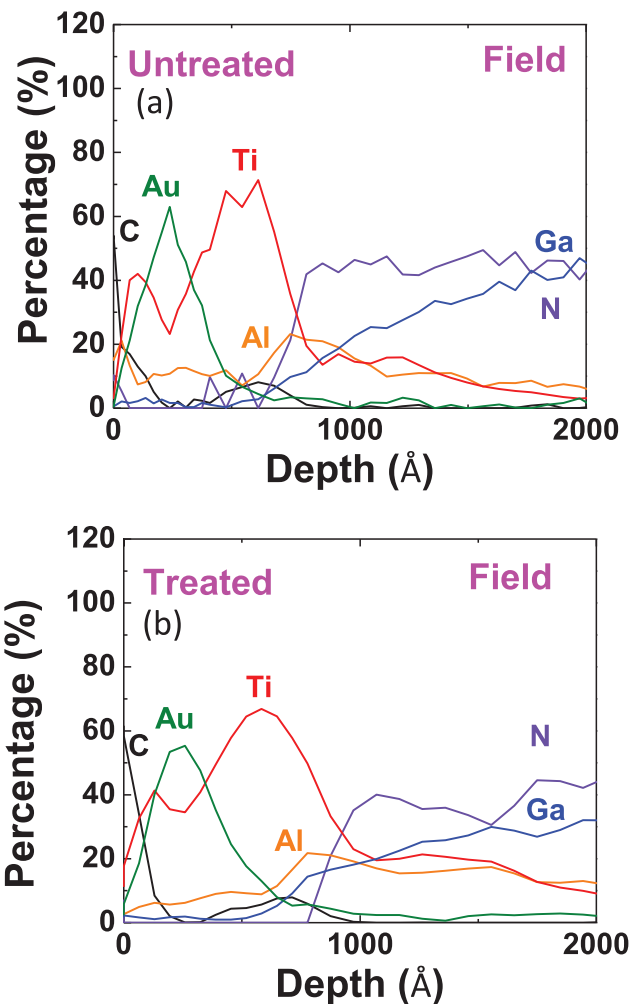


Fig. 8. (Color online) Auger depth profile of the field region of (a) an untreated sample and (b) BOE treated sample.

observed for the untreated sample. Zhou *et al.* reported that TiN-based contact inclusion (CIs) form at the GaN surface.⁸ The diameter and density of CIs were around 100 nm and $2 \times 10^{-7}/\text{cm}^2$, respectively. The Auger beam spot size used in this study was around 35 nm. Thus, it is possible that the CI region might be missed during the Auger depth profiling for the untreated sample.

Figure 7(a) shows Auger depth profile of the ring area for the untreated sample. There was a surface layer containing C, O, Ti, and Al, followed with a Ti layer mixed with Au-Al alloy layer, a thicker Au-Al layer, and an interface layer between Au-Al-Ti alloy layer and GaN. After BOE-treatment, not only was the surface Al was removed, but also some Ti and Au-Al alloyed layers were etched off, as shown in Fig. 7(b). This is consistent with EDX data which Au decreased around 7%. Although Au is quite stable with acid solution, the etching of surface Al and Al in Au-Al alloy layers might take away Au. The removal of Au on these surface layers increased the Ohmic metallization sheet resistance.

Figure 8 shows the Auger depth profiles of the field region of (a) an untreated sample and (b) BOE treated sample. There was a similar surface layer as the one on island and ring areas, containing C, O, Ti, and Al, followed with a Ti layer mixed with Au-Al alloy layer, a Ti layer on the top of GaN. After treatment, the surface Al was etched off. There were no changes on the other layers.

IV. CONCLUSIONS

The degradation of Ohmic metallization dipped in BOE was studied. The sheet resistance of Ohmic metallization increased significantly after treatment in BOE for 3 min. Moreover, after annealing, there were island-like structures surrounded by Au-Al alloy rings and a field area between the islands. The BOE etching occurred mainly at the island and ring areas instead of the field area between the islands. The increase of sheet resistance was due to the etching of surface

Al and Ti and the loss of Au in the island and ring areas. To minimize BOE exposure time, CF_4/O_2 plasma can be used to etch off the majority of the dielectric, then use BOE treatment to remove the rest of the dielectric to prevent plasma ion bombardment damage.

ACKNOWLEDGMENTS

The work performed at UF is supported by an U.S. DOD HDTRA Grant No. 1-11-1-0020 monitored by James Reed and a NSF Grant No. ECCS-1445720 monitored by John Zavada. A portion of this research was conducted at the Center for Nanophase Materials Sciences, which is a DOE Office of Science User Facility. The authors would like to thank Pat McKeown in Evans Analytical Group for very fruitful discussion of Auger results.

¹Y.-F. Wu, A. Saxler, M. Moore, R. Smith, S. Sheppard, P. Chavarkar, T. Wisleder, U. Mishra, and P. Parikh, *IEEE Electron Device Lett.* **25**, 117 (2004).

²H. Sun, A. Alt, H. Benedickter, and C. Bolognesi, *IEEE Electron Device Lett.* **45**, 376 (2009).

³Y. Wei, Z. Renping, D. Yandong, H. Weihua, and Y. Fuhua, *J. Semicond.* **33**, 064005 (2012).

⁴G. S. May and S. M. Sze, *Fundamental of Semiconductor Fabrication*, 1st ed. (Wiley, New York, 2003), pp. 87–88.

⁵J. Algueperse, P. Mollard, D. Devilliers, M. Chemla, R. Faron, R. Romana, and J. P. Cuer, *Ullmann's Encyclopedia of Industrial Chemistry* (Wiley, New York, 2005).

⁶K. R. Williams and R. S. Muller, *J. Microelectromech. Syst.* **5**, 256 (1996).

⁷K. R. Williams, K. Gupta, and M. Wasilik, *J. Microelectromech. Syst.* **12**, 761 (2003).

⁸L. Zhou, J. H. Leach, X. Ni, H. Morkoc, and D. J. Smith, *J. Appl. Phys.* **107**, 14508 (2010).

⁹Z. Yue-Zong, F. Shi-Wei, G. Chun-Sheng, Z. Guang-Chen, Z. Si-Xiang, S. Rong, B. Yun-Xia, and L. Chang-Zhi, *Chin. Phys. Lett.* **25**, 4083 (2008).

¹⁰C.-F. Lo, L. Liu, C. Y. Chang, F. Ren, V. Craciun, S. J. Pearton, Y. W. Heo, O. Laboutin, and J. W. Johnson, *J. Vac. Sci. Technol. B* **29**, 021002 (2011).